

# Cerebral Dynamics and Metabolism of Hyperpolarized [1-13C] Pyruvate using Time Resolved Spiral-Spectroscopic Imaging

R. E. Hurd<sup>1</sup>, D. Mayer<sup>2,3</sup>, Y-F. Yen<sup>1</sup>, J. Tropp<sup>1</sup>, A. Pfefferbaum<sup>2,4</sup>, and D. Spielman<sup>3</sup>

<sup>1</sup>Applied Sciences Laboratory, GE Healthcare, Menlo Park, CA, United States, <sup>2</sup>SRI International, <sup>3</sup>Radiology, Stanford, <sup>4</sup>Psychiatry and Behavioral Sciences, Stanford

## Introduction

MR metabolic imaging of hyperpolarized [1-<sup>13</sup>C]-pyruvate is a useful tool in the study of oncology and cardiology (1,2). Dynamic and tissue level changes in [1-<sup>13</sup>C]-pyruvate and its metabolic products, [1-<sup>13</sup>C]-lactate, [1-<sup>13</sup>C]-alanine and [<sup>13</sup>C] bicarbonate, have been shown to correlate with metabolic states of interest including disease progression (3) and response to therapy (4,5). However, because of the very limited 1-2 minute lifetime of hyperpolarized signal in vivo, brain metabolism has been largely ignored as an application. Although the kinetics of blood-brain transport of pyruvate (6-8), are a limit, single time point images have been reported, showing pyruvate uptake, and metabolism, in normal anesthetized rat brain (9). Brain levels of labeled pyruvate are substantially less than blood levels, but are sufficient to map lactate distribution. Labeled lactate and bicarbonate, generated from hyperpolarized [1-<sup>13</sup>C]-pyruvate transported into brain, can be directly measured. However, without prior knowledge of the shape and position of the bolus relative to the imaging window, it was not possible to separate [1-<sup>13</sup>C]-pyruvate in the brain parenchyma from [1-<sup>13</sup>C]-pyruvate in the cerebral blood volume (CBV). In this study, fast 125 msec dynamic imaging (10) is used to better characterize the bolus, transport and metabolic effects, separating the metabolites in the cerebral blood volume from the metabolites in brain tissue.

## Material and Methods

**Animal Preparation:** The experiments were performed on 5 healthy (197-257 g) male Wistar rats anesthetized with 1-3% isoflurane in oxygen (~1.5 L/min). Respiration, rectal temperature, heart rate, and oxygen saturation were monitored throughout the experiment. Rectal temperature was kept at 37 °C by heating the animal with a temperature-controlled warm water blanket. Hyperpolarized solution was injected via tail vein catheter. Each rat was injected 3 times at a 1.5-hour interval and images collected. Preparation and physiological monitoring of the animals in the <sup>13</sup>C experiment followed the protocol approved by the local Institutional Animal Care and Use Committees.

**Hyperpolarized [1-<sup>13</sup>C] pyruvate:** Hyperpolarized solutions of [1-<sup>13</sup>C]-pyruvate were prepared as described previously (11) using a HyperSense™ polarizer (Oxford Instruments Molecular Biotools, Oxford, UK). All rats were injected with 80 mM pyruvate. The level of liquid state polarization was estimated from solid-state DNP build up levels. A calibration of the solid-state DNP level with liquid-state polarization was made on the 3T scanner using the pyruvate thermal equilibrium signal as well as the thermal equilibrium signal of an 8 M <sup>13</sup>C-urea standard. Liquid-state polarization levels ranged from 22-26%. The pyruvate T<sub>1</sub> at 3T and apparent T<sub>1</sub> during the low field transfer process were also determined to help estimate losses between dissolution and injection. The time delay between dissolution to injection into the animal ranged from 23 – 25 s. The total rat dose ranged from 2.4 – 3mL of 80mM pyruvate, injected over 12s.

**MR Hardware and Methods:** All experiments were performed on a 3T Signa™ (GE Healthcare, Waukesha, WI) equipped with a high-performance insert gradient coil (500 mT/m). A custom-built dual-tuned (<sup>1</sup>H/<sup>13</sup>C) quadrature rodent coil (inner diameter: 50mm), operating at 127.7 MHz and 32.1 MHz, respectively, was used for both RF excitation and signal reception.

**<sup>13</sup>C Spiral Imaging:** In-plane axial resolution was 2.7mm x 2.7mm with a slice of 10mm. 125ms images were sampled every 3s starting at 9s from start of injection.

**Standard Reference:** A reference phantom, 800µL in a sealed 1mL plastic syringe barrel, was constructed using 8 M <sup>13</sup>C-Urea in 80:20 w/w water:glycerol. T<sub>1</sub> was adjusted to 1s with 3 µL/mL Gd-chelate, (OmniScan™, GE Healthcare Oslo).

## Results

Dynamic pyruvate and lactate metabolic images are shown in Figure 1. Each of the individual pyruvate (left) and lactate (right) images, were averaged over 3 injections into the same animal. At the bottom of the figure, pyruvate (left) and lactate (right) images, averaged over 8 time points between 21 and 42 s are overlaid on a proton anatomic image. In these time-averaged images, the lactate signal is scaled to the pyruvate level. The time course for lactate (red) and pyruvate (green) in brain, along with the dynamics of an intravascular pyruvate (blue) ROI are shown. Figure 2 illustrates repeatability between two subjects, and compares the dynamics to a model based on A) cerebral blood volume of 3.6% (12) and B) pyruvate blood-to-brain transport kinetics reported by Partridge (8); V<sub>max</sub> = 88 nmol min<sup>-1</sup> g<sup>-1</sup> and K<sub>d</sub> = .034 mL min<sup>-1</sup> g<sup>-1</sup>. Figure 3 compares an average of all runs relative to a model in which the “brain” pyruvate is assumed to be primarily from cerebral blood volume (i.e. LDH is assumed to be fast relative to pyruvate transport). Intravascular pyruvate T<sub>1</sub> (13) and a 14% min<sup>-1</sup> lactate exchange across the blood brain barrier (14) are also included in this model.

## Discussion

In all 14 individual runs, the lactate response is very consistent and represents the bulk of the <sup>13</sup>C label in brain. The blood-to-brain transport of pyruvate is sufficient to label 350±/35 nmol g<sup>-1</sup> of the lactate pool. A brain model in which the labeled pyruvate is dominated by CBV contributions, and labeled lactate is dominated by brain tissue, best fits the observed dynamic metabolic images. This suggests that we can measure transport and steady state lactate levels, but not LDH kinetics under these conditions. The time averaged images are equivalent in SNR and image quality to the single point 20 s CSI images previously reported (9), but have the advantage of resolving the effect of the bolus shape and its impact on lactate/pyruvate estimates.

**Acknowledgments** NIH grants RR09784, AA05965, AA13521-INIA, and EB009070.

**References** 1. Golman et al.(2006) *Cancer Res* 66:10855, 2. Golman et al.(2008) *Magn Reson Med*. 59:1005, 3. Albers et al.(2008) *Cancer Res* 68:8607, 4. Chen et al.(2008) *Proc 16<sup>th</sup> Annual ISMRM*, p. 888, 5. Day et al.(2007) *Nature Medicine* 13:1382 6. Cremer et al.(1979) *J. Neurochem* 33:439, 7. Miller and Oldendorf (1986) *J. Neurochem*. 46:1412, 8. Partridge (1983) *American Physiol. Soc.* 63:1481, 9. Hurd et al (2009) *Proc 17<sup>th</sup> Annual ISMRM* p. 56, 10. Mayer et al.(2009) *MRM* 62:557, 11. Kohler et al.(2007) *MRM*. 58:65, 12. Julien-Dolbec et al.(2002) *Br J. Anaest* 89:287, 13. Leung et al.(2009) *Proc 17<sup>th</sup> Annual ISMRM* p. 2432, 14 Lear and Kasliwal(1991) *JCBFM* 11:576.

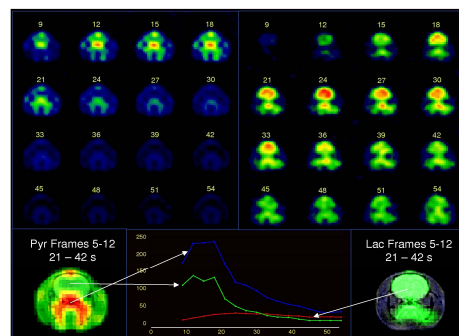


Figure 1. Dynamic images and time course: top left panel: individual pyruvate images and top right panel: individual lactate images.

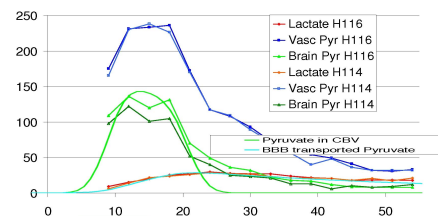


Figure 2. Metabolite time course for two subjects, and fit to a first pass of the bolus through CBV and expected BBB transport

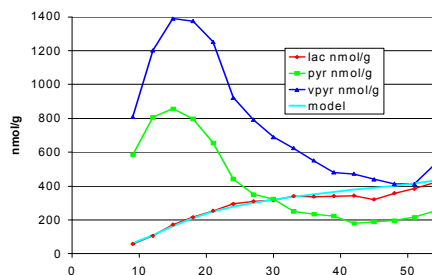


Figure 3. CBV pyruvate model. Observed lactate (red) vs model prediction (light blue)